

Thermal rectification properties of multiple-quantum-dot junctions

David M.-T. Kuo¹ and Yia-chung Chang²

¹*Department of Electrical Engineering and Department of Physics,
National Central University, Chungli, 320 Taiwan and*

²*Research Center for Applied Sciences, Academic Sinica, Taipei, 115 Taiwan
(Dated: February 14, 2022)*

It is illustrated that semiconductor quantum dots (QDs) embedded into an insulating matrix connected with metallic electrodes and some vacuum space can lead to significant thermal rectification effect. A multilevel Anderson model is used to investigate the thermal rectification properties of the multiple-QD junction. The charge and heat currents in the tunneling process are calculated via the Keldysh Green's function technique. We show that pronounced thermal rectification and negative differential thermal conductance (NDTC) behaviors can be observed for the multiple-QD junction with asymmetrical tunneling rates and strong interdot Coulomb interactions.

Records of thermal rectification date back to 1935 when Starr discovered that copper oxide/copper junctions can display a thermal diode behavior.¹ Recently, thermal rectification effects have been predicted to occur in one dimensional phonon junction systems.^{2–5} Such a thermal rectification effect is crucial for heat storage. Scheibner and coworkers have experimentally observed the asymmetrical thermal power of the two-dimensional electron gas in QD under high magnetic fields.⁶ So far the rectification mechanism of a single QD is still ambiguous owing to the unclear relation between the thermal power and the thermal rectification effect. This inspires us to investigate whether the QD junction system can act as a thermal rectifier. A useful thermal diode to store solar heating energy not only requires a high rectification efficiency but also high heat flow. The later requires a high QD density in the QD junction thermal diode. The main goal of this study is to illustrate that the multiple QDs embedded into an insulator connected with metallic electrodes and with a vacuum layer insert can give rise to significant thermal rectification and negative differential thermal conductance (NDTC) effects in the nonlinear response regime. We also clarify the relation between the thermal power and the rectification effect.

The proposed insulator/quantum dots/vacuum (IQV) double barrier tunnel junction system (as illustrated in Fig. 1) can be adequately described by a multi-level Anderson model.⁷ Here, the vacuum layer serves as a blocking layer for phonon contributions to thermal conduction, while allowing electrons to tunnel through. We assume that the energy level separation between the ground state and the first excited state within each QD is much larger than $k_B T$, where T is the temperature of concern. Therefore, there are only one energy level for each QD. We have ignored the interdot hopping terms due to the high potential barrier separating QDs. The key effects included are the intradot and interdot Coulomb interactions and the coupling between the QDs with the metallic leads. Using the Keldysh-Green's function technique,⁸ the charge and heat currents through the junction can be expressed as

$$J_e = \frac{-2e}{h} \sum_{\ell} \int d\epsilon \gamma_{\ell}(\epsilon) \text{Im} G_{\ell,\sigma}^r(\epsilon) f_{LR}(\epsilon), \quad (1)$$

$$Q = \frac{-2}{h} \sum_{\ell} \int d\epsilon \gamma_{\ell}(\epsilon) \text{Im} G_{\ell,\sigma}^r(\epsilon) (\epsilon - E_F - e\Delta V) f_{LR}(\epsilon), \quad (2)$$

where $\gamma_{\ell}(\epsilon) = \frac{\Gamma_{\ell,L}(\epsilon)\Gamma_{\ell,R}(\epsilon)}{\Gamma_{\ell,L}(\epsilon)+\Gamma_{\ell,R}(\epsilon)}$ is the transmission factor. $f_{LR}(\epsilon) = f_L(\epsilon) - f_R(\epsilon)$ and $f_{L(R)}(\epsilon) = 1/(exp^{(\epsilon-\mu_{L(R)})/(k_B T_{L(R)})} + 1)$ is the Fermi distribution function for the left (right) electrode. The chemical potential difference between these two electrodes is related to the bias difference $\mu_L - \mu_R = e\Delta V$ created by the temperature gradient. $T_L(T_R)$ denotes the temperature maintained at the left (right) lead. $E_F = (\mu_L + \mu_R)/2$ denotes the average Fermi energy of the electrodes. $\Gamma_{\ell,L}(\epsilon)$ and $\Gamma_{\ell,R}(\epsilon)$ [$\Gamma_{\ell,\beta} = 2\pi \sum_{\mathbf{k}} |V_{\ell,\beta,\mathbf{k}}|^2 \delta(\epsilon - \epsilon_{\mathbf{k}})$] denote the tunneling rates from the QDs to the left and right electrodes, respectively. e and h denote the electron charge and Planck's constant, respectively. For simplicity, these tunneling rates are assumed to be energy- and bias-independent. Eqs. (1) and (2) have been employed to study the thermal properties of single-level QD in the Kondo regime.⁹ Here, our analysis is devoted to the multiple-QD system in the Coulomb blockade regime. The expression of the retarded Green function for dot ℓ of a multi-QD system, $G_{\ell,\sigma}^r(\epsilon)$ can be found in Ref. [7]

To study the direction-dependent heat current, we let $T_L = T_0 + \Delta T/2$ and $T_R = T_0 - \Delta T/2$, where $T_0 = (T_L + T_R)/2$ is the equilibrium temperature of two side electrodes and $\Delta T = T_L - T_R$ is the temperature difference. Because the electrochemical potential difference, $e\Delta V$ yielded by the thermal gradient could be significant, it is important to keep track the shift of the energy level of each dot according to $\epsilon_{\ell} = E_{\ell} + \eta_{\ell} \Delta V/2$, where η_{ℓ} is the ratio of the distance between dot ℓ and the mid plane of the QD junction to the junction width. Here we set $\eta_B = \eta_C = 0$. A functional thermal rectifier requires a good thermal conductance for $\Delta T > 0$, but a poor thermal conductance for $\Delta T < 0$. Based on Eqs. (1) and (2), the asymmetrical behavior of heat current with respect to ΔT requires not only highly asymmetric coupling strengthes between the QDs and the electrodes but also strong electron Coulomb interactions between dots. To investigate the thermal rectification behavior, we have numerically solved Eqs. (1) and (2) for multiple-

QD junctions involving two QDs and three QDs for various system parameters. We first determine ΔV by solving Eq. (1) with $J_e = 0$ (the open circuit condition) for a given ΔT , T_0 and an initial guess of the average one-particle and two-particle occupancy numbers, N_ℓ and c_ℓ for each QD. Those numbers are then updated according to Eqs. (5) and (6) in Ref. [7] until self-consistency is established. For the open circuit, the electrochemical potential will be formed due to charge transfer generated by the temperature gradient. This electrochemical potential is known as the Seebeck voltage (Seebeck effect). Once ΔV is solved, we then use Eq. (2) to compute the heat current.

Fig. 2 shows the heat currents, occupation numbers, and differential thermal conductance (DTC) for the two-QD case, in which the energy levels of dot A and dot B are $E_A = E_F - \Delta E/5$ and $E_B = E_F + \alpha_B \Delta E$, where α_B is tuned between 0 and 1. The heat currents are expressed in units of $Q_0 = \Gamma^2/(2h)$ through out this article. The intradot and interdot Coulomb interactions used are $U_\ell = 30k_B T_0$ and $U_{AB} = 15k_B T_0$. The tunneling rates are $\Gamma_{AR} = 0$, $\Gamma_{AL} = 2\Gamma$, and $\Gamma_{BR} = \Gamma_{BL} = \Gamma$. $k_B T_0$ is chosen to be 25Γ throughout this article. Here, $\Gamma = (\Gamma_{AL} + \Gamma_{AR})/2$ is the average tunneling rate in energy units, whose typical values of interest are between 0.1 and 0.5 meV. The dashed curves are obtained by using a simplified expression of Eq. (2) in which we set the average two particle occupation in dots A and B to zero (resulting from the large intradot Coulomb interactions) and taking the limit that $\Gamma \ll k_B T_0$ so the Lorentzian function of resonant channels can be replaced by a delta function. We have

$$Q/\gamma_B = \pi(1 - N_B)[(1 - 2N_A)(E_B - E_F)f_{LR}(E_B) + 2N_A(E_B + U_{AB} - E_F)f_{LR}(E_B + U_{AB})],$$

Here $N_{A(B)}$ is the average occupancy in dot A(B). Therefore, it is expected that the curve corresponding to $E_B = E_F + 4\Delta E/5$ obtained with this delta function approximation is in good agreement with the full solution, since E_B is far away from the Fermi energy level. For cases when E_B is close to E_F , the approximation is not as good, but it still gives qualitatively correct behavior. Thus, it is convenient to use this simple expression to illustrate the thermal rectification behavior. The asymmetrical behavior of N_A with respect to ΔT is mainly resulted from the condition $\Gamma_{AR} = 0$ and $\Gamma_{AL} = 2\Gamma$. The heat current is contributed from the resonant channel with $\epsilon = E_B$, because the resonant channel with $\epsilon = E_B + U_{AB}$ is too high in energy compared with E_F . The sign of Q is determined by $f_{LR}(E_B)$, which indirectly depends on Coulomb interactions, tunneling rate ratio and QD energy levels. The rectification behavior of Q is dominated by the factor $1 - 2N_A$, which explains why the energy level of dot-A should be chosen below E_F and the presence of interdot Coulomb interactions is crucial. The negative sign of Q in the regime of $\Delta T < 0$ indicates that the heat current is from the right electrode to the left electrode. We define the rectification efficiency as

$\eta_Q = (Q(\Delta T = 30\Gamma) - |Q(\Delta T = -30\Gamma)|)/Q(\Delta T = 30\Gamma)$. We obtain $\eta_Q = 0.86$ for $E_B = E_F + 2\Delta E/5$ and 0.88 for $E_B = E_F + 4\Delta E/5$. Fig. 2(c) shows DTC in units of $Q_0 k_B/\Gamma$. It is found that the rectification behavior is not very sensitive to the variation of E_B . DTC is roughly linearly proportional to ΔT in the range $-20\Gamma < k_B \Delta T < 20\Gamma$. In addition, we also find a small negative differential thermal conductance (NDTC) for $E_B = E_F + 4\Delta E/5$. Similar behavior was reported in the phonon junction system.¹⁰

Fig. 3 shows the heat current, differential thermal conductance and thermal power ($S = e\Delta V/k_B \Delta T$) as functions of temperature difference ΔT for a three-QD case for various values of Γ_{AR} , while keeping $\Gamma_{B(C),R} = \Gamma_{B(C),L} = \Gamma$. Here, we adopt $\eta_A = |\Gamma_{AL} - \Gamma_{AR}|/(2\Gamma)$ instead of fixing η_A at 0.3 to reflect the correlation of dot position with the asymmetric tunneling rates. We assume that the three QDs are roughly aligned with dot A in the middle. The energy levels of dots A, B and C are chosen to be $E_A = E_F - \Delta E/5$, $E_B = E_F + 2\Delta E/5$ and $E_C = E_F + 3\Delta E/5$. $U_{AC} = U_{BA} = 15k_B T_0$, $U_{BC} = 8k_B T_0$, $U_C = 30k_B T_0$, and all other parameters are kept the same as in the two-dot case. The thermal rectification effect is most pronounced when $\Gamma_{AR} = 0$, as seen in Fig. 4(a). (Note that the heat current is not very sensitive to U_{BC}). In this case, we obtain a small heat current $Q = 0.068Q_0$ at $\Delta T = -30\Gamma$, but a large heat current $Q = 0.33Q_0$ at $\Delta T = 30\Gamma$ and the rectification efficiency η_Q is 0.79. However, the heat current for $\Gamma_{AR} = 0$ is small. For $\Gamma_{AR} = 0.1\Gamma$, we obtain $Q = 1.69Q_0$ at $\Delta T = -30\Gamma$, $Q = 5.69Q_0$ at $\Delta T = 30\Gamma$, and $\eta_Q = 0.69$. We see that the heat current is suppressed for $\Delta T < 0$ with decreasing Γ_{AR} . This implies that it is important to blockade the heat current through dot A to observe the rectification effect. Very clear NDTC is observed in Fig. 3(b) for the $\Gamma_{AR} = 0.1\Gamma$ case, while DTC is symmetric with respect to ΔT for the $\Gamma_{AR} = \Gamma_{AL}$ case.

From the experimental point of view, it is easier to measure the thermal power than the direction-dependent heat current. The thermal power as a function of ΔT is shown in Fig. 3(c). All curves except the dash-dotted line (which is for the symmetrical tunneling case) show highly asymmetrical behavior with respect to ΔT , yet it is not easy at all to judge the efficiency of the rectification effect from S for small $|\Delta T|$ ($k_B |\Delta T|/\Gamma < 10$). Thus, it is not sufficient to determine whether a single QD can act as an efficient thermal rectifier based on results obtained in the linear response regime of $\Delta T/T_0 \ll 1$.⁶ According to the thermal power values, the electrochemical potential $e\Delta V$ can be very large. Consequently, the shift of QD energy levels caused by ΔV is quite important. To illustrate the importance of this effect, we plot in Fig. 4 the heat current for various values of E_C for the case with $\Gamma_{AR} = 0$, $U_{BC} = 10k_B T_0$ and $\eta_A = 0.3$. Other parameters are kept the same as those for Fig. 3. The solid (dashed) curves are obtained by including (excluding) the energy shift $\eta_A \Delta V/2$. It is seen that the shift of QD energy levels due

to ΔV can lead to significant change in the heat current. It is found that NDTC is accompanied with low heat current for the case of $E_C = E_F + \Delta E/5$ [see Fig. 4(b)]. Even though the heat currents exhibits rectification effect for $E_C = E_F + \Delta E/5$ and $E_C = E_F + 3\Delta E/5$, the thermal powers have very different behaviors. From Figs. 3(c) and 4(c), we see that the heat current is a highly non-linear function of electrochemical potential ΔV . Consequently, the rectification effect is not straightforwardly related to the thermal power in this system.

Comparing the heat currents of the three-dot case (shown in Figs. 3 and 4) to the two-dot case (shown in Fig. 2), we find that the rectification efficiency is about the same for both cases, while the magnitude of the heat current can be significantly enhanced in the three-dot case. For practical applications, we need to estimate the magnitude of the heat current density and DTC of the IQV junction device in order to see if the effect is significant. We envision a thermal rectification device made of an array of multiple QDs (e.g. three-QD cells) with a 2D density $N_{2d} = 10^{11} \text{cm}^{-2}$. For this device, the heat

current density versus ΔT is given by Figs. 3 and 4 with the units Q_0 replaced by $N_{2d}Q_0$, which is approximately 965W/m^2 if we assume $\Gamma = 0.5 \text{meV}$. Similarly, the units for DTC becomes $N_{2d}k_B Q_0/\Gamma$, which is approximately $34 \text{W/}^0\text{Km}^2$. Since the phonon contribution can be blocked by the vacuum layer in our design, this device should have practical applications near 140^0K with ($k_B T_0 \approx 12.5 \text{meV}$). If we choose a higher tunneling rate $\Gamma > 1 \text{meV}$ and Coulomb energy $> 300 \text{meV}$ (possible for QDs with diameter less than 1 nm), then it is possible to achieve room-temperature operation.

In summary, we have reported a design of multiple-QD junction which can have significant thermal rectification effect. The thermal rectification behavior is sensitive to the coupling between the QDs and the electrodes, the electron Coulomb interactions and the energy level differences between the dots.

Acknowledgments

This work was supported by Academia Sinica, Taiwan.

Email-address: mtkuo@ee.ncu.edu.tw; yichang@gate.sinica.edu.tw

-
- ¹ C. Starr, J. Appl. Phys. 7, **15** (1936).
 - ² M. Terraneo, M. Peyrard, G. Casati, Phys. Rev. Lett. **88**, 094302 (2002).
 - ³ Baowen Li, L. Wang and G. Casati, Phys. Rev. Lett. **93**, 184301 (2004).
 - ⁴ B. Hu, L. Yang and Y. Zhang, Phys. Rev. Lett. **97**, 124302 (2006).
 - ⁵ N. Yang, G. Zhang and B. Li, Appl. Phys. Lett. **95**, 033107 (2009).
 - ⁶ R. Scheibner, M. König, D. Reuter, A. D. Wieck, C. Gould, H. Bühmann and L. W. Molenkamp, New. J. Phys. **10**, 083016 (2008).
 - ⁷ D. M. T. Kuo and Y. C. Chang, Phys. Rev. Lett. **99**, 086803 (2007).
 - ⁸ H. Haug and A. P. Jauho, *Quantum Kinetics in Transport and Optics of Semiconductors* (Springer, Heidelberg, 1996).
 - ⁹ M. Krawiec and K. I. Wysokiński, Phys. Rev. B **75**, 155330 (2007).

- ¹⁰ D. Segal, Phys. Rev. B **73**, 205415 (2006).

Figure Captions

Fig. 1. Schematic diagram of the insulator/quantum dots/vacuum tunnel junction device.

Fig. 2. (a) Heat current (b) average occupation number, and (c) differential thermal conductance as a function of ΔT for various values of E_B for a two-QD junction. $\Gamma_{AR} = 0$, $\eta_A = 0.3$ and $\Delta E = 200\Gamma$.

Fig. 3. (a) Heat current, (b) differential thermal conductance and (c) thermal power as a function of ΔT for various values of Γ_{AR} for a three-QD junction.

Fig. 4. (a) Heat current, (b) differential thermal conductance and (c) thermal power as functions of ΔT for various values of E_C for a three-QD junction with $\Gamma_{AR} = 0$ and $\eta_A = 0.3$.

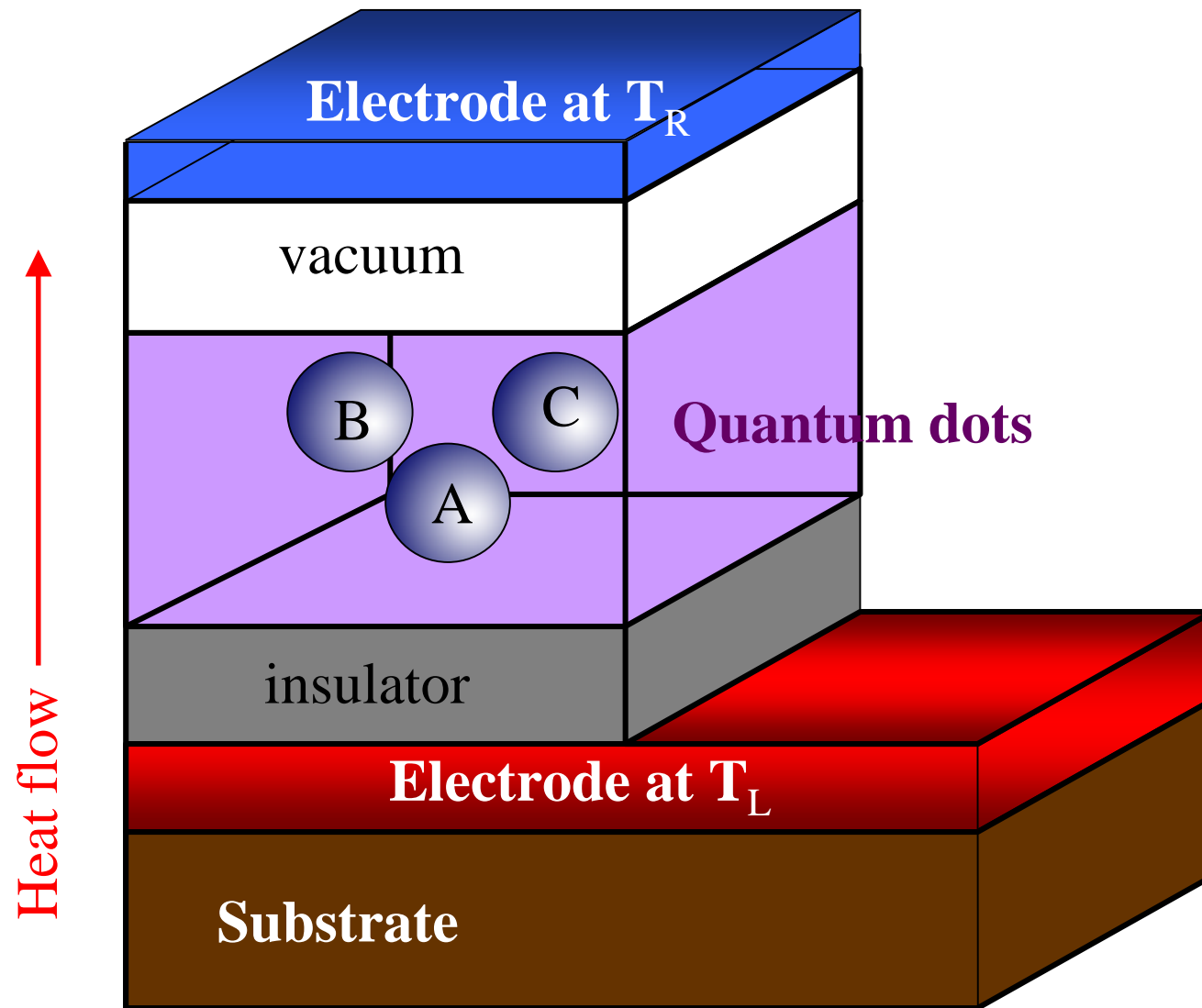


Fig. 1

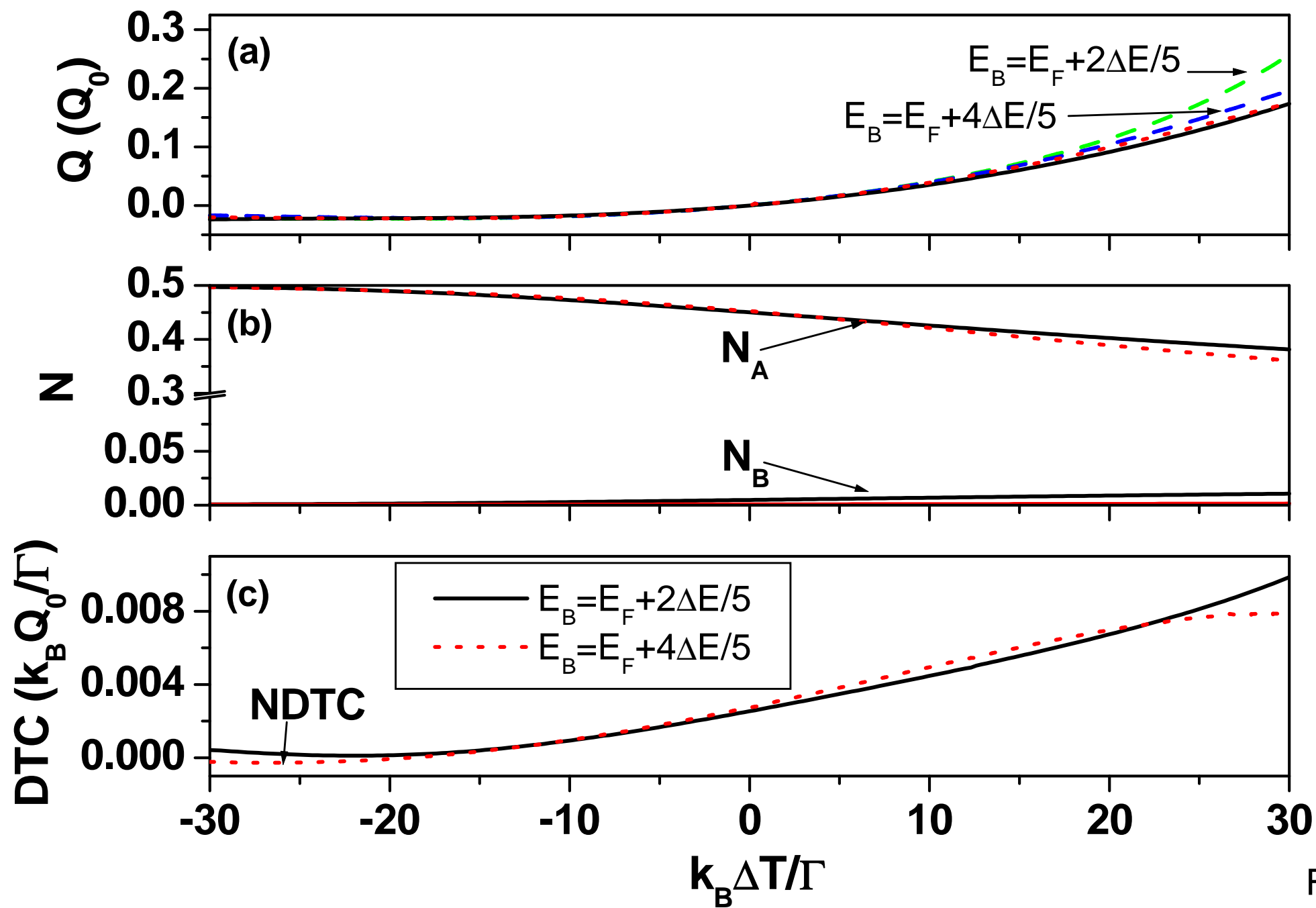


Fig2

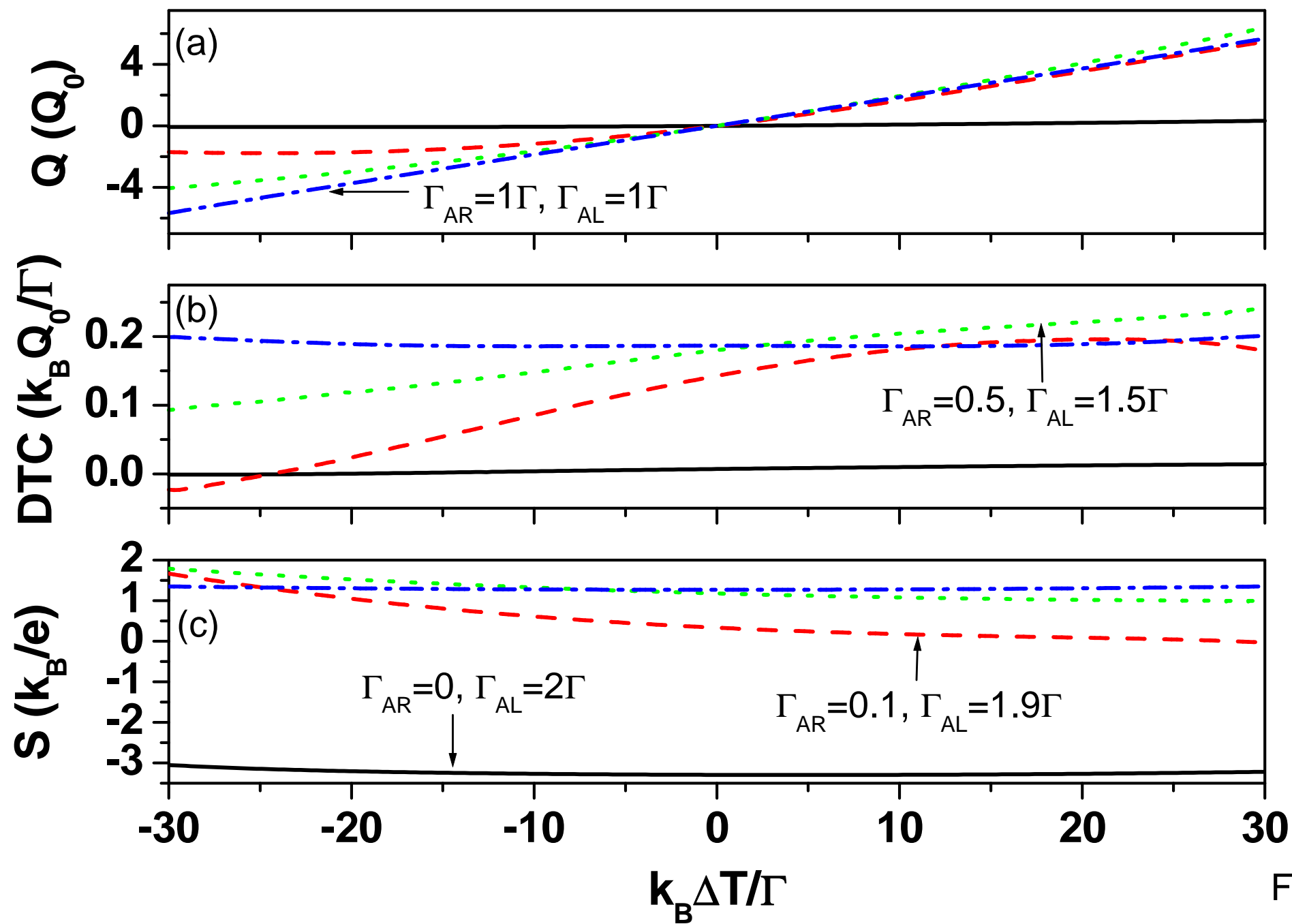


Fig3

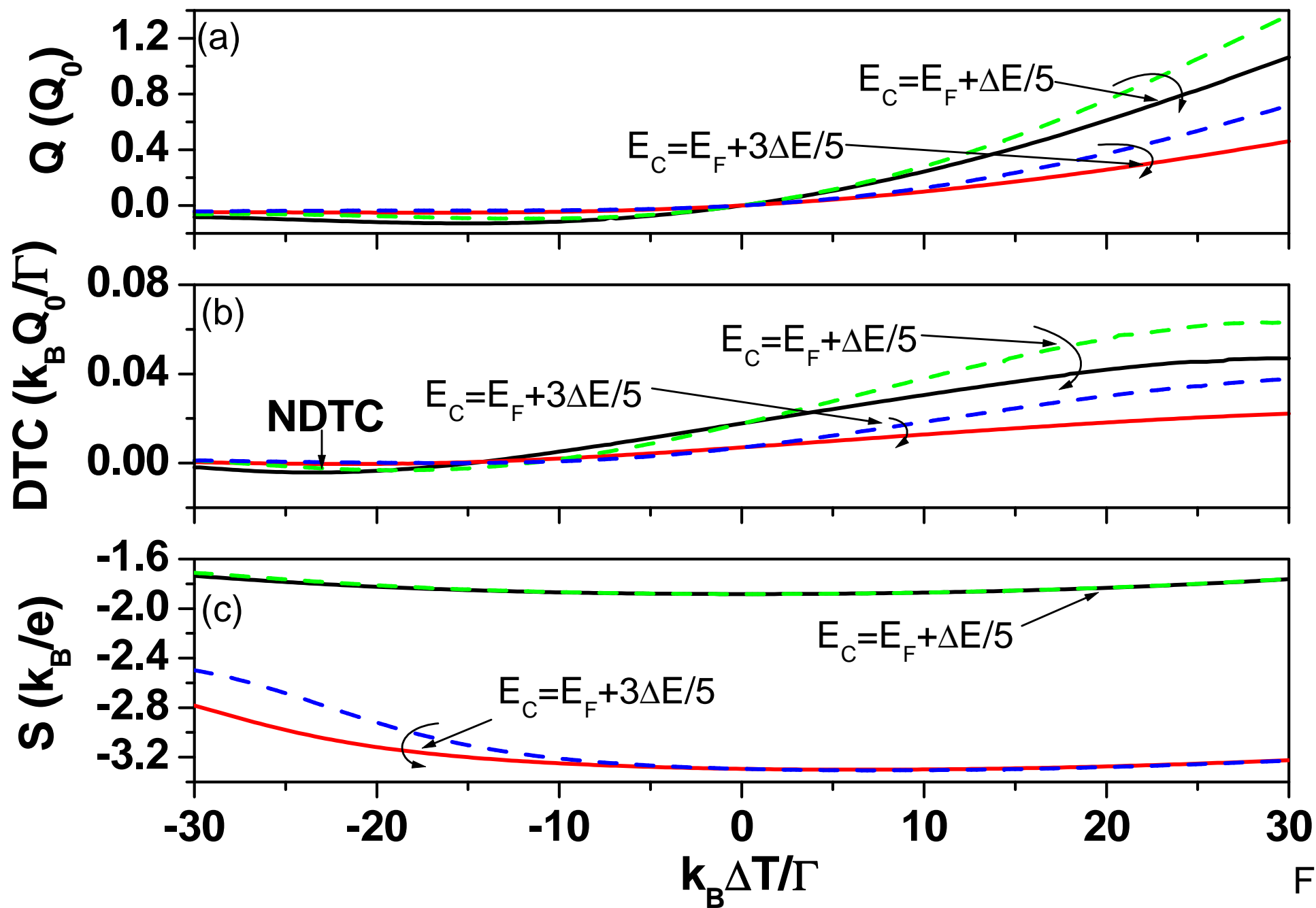


Fig4